Friction fatigue in weak rock and non-cohesive soils with soft grains: a physical model for the role of abrasive wear in skin friction reduction

Jort van Wijk, PhD MSc [i)]

i) Manager Geotechnical Advisory Services, IQIP, Molendijk 94, 3361 EP Sliedrecht, The Netherlands.

ABSTRACT

Friction fatigue, the progressive reduction in shaft resistance at a certain soil horizon upon penetration of the pile, for sandy soils is related to the relative penetration and the cyclic nature of pile driving. Friction fatigue is also known in weak rock (e.g. chalk) or cemented soils with soft grains. Contrary to steel-sand interfaces, steel-chalk interfaces are reported to produce a low strength putty under cyclic loading and shearing. In this article we present a physical model for friction fatigue in weak rock based on abrasive wear theory, including the development of an intermediate interface layer and the mechanical/rheological properties of the interface layer. The model is verified with experimental data from literature (interface shear tests with chalk and calcareous sands). The model describes the reduction in interface friction well. Validation with well-documented cases of pile driving will be part of future work.

Keywords: friction fatigue, abrasive wear, weak rock, cemented soils

1 INTRODUCTION

Empirical relations exist for including friction fatigue in SRD models for sandy and clayey soils (Alm and Hamre, 2001; Jardine et al. 2005; Lehane et al. 2005; Barrett and Prendergast, 2020), and the underlying physics (e.g. grain contraction at the interface, cyclic loading) are understood (White and Lehane, 2004; Gavin and O'Kelly, 2007; Beijer-Lundber, 2009).

Terente et al. (2015,2017) focus on friction fatigue in weak rock in general and relate it to the UCS. In cemented calcareous sands friction fatigue is associated with destruction of soil matrices and successive grain crushing (Tabucanon, 1997; Poulos, 2000; Denes, 2016). In chalk a putty develops at the pile shaft that reduces friction (Jardine et al., 2018 and references therein; Buckley, 2018).

While for sands and clays the physics of friction fatigue are well-investigated, this is not the case for weak rock. This article aims at improving the understanding of friction fatigue in weak rock by presenting a physical model that considers particle crushing due to sliding (abrasive) wear, reduction in normal stress on the wear surface and development of a paste interface-layer which directly relates to the relative pile penetration.

2 WEAR MECHANISMS AT THE PILE-SOIL INTERFACE

Sliding of the pile against the soil causes friction and wear. The sliding wear occurring at the pile-soil interface is predominantly governed by mechanical properties of both the soil/rock and the pile, and to a lesser extent by chemical activity and thermal effects (Hutchings and Shipway, 2017). The ability of one body to wear out the other is determined by the relative hardness of both materials. On Mohs hardness scale quartz (Mohs 7, which is the dominant mineral in most sandy soils) and engineering steels have comparable hardness (Mohs 6-8). Both materials affect each other during sliding and one would observe the quartz minerals 'polishing' the steel pile. The minerals themselves will hardly be affected by the smooth pile due to the lack of asperities on the pile, which explains why friction fatigue in sandy soils is dominated by granular contraction rather than abrasion of the grains (although grain crushing at the pile toe and the relative displacement of the crushed grains along the shaft as the pile penetrates cannot be discarded, these fines are not directly related to abrasive wear).

Minerals as talc, gypsum and calcite all show Mohs < 5, which implies that soils and rocks consisting of these or similar minerals are much more susceptible to wear by steel piles. The pile will largely wear down the rock in a three-body wear system, ultimately resulting in smooth rock surfaces. The abraded particles will form a powder cake in case of dry rock, or will form a putty in saturated conditions.

Fig.1 shows how the different processes at the pile-soil interface are determined by the mechanical and environmental properties of the system. Three cases A, B and C are be described by the theory in this paper.

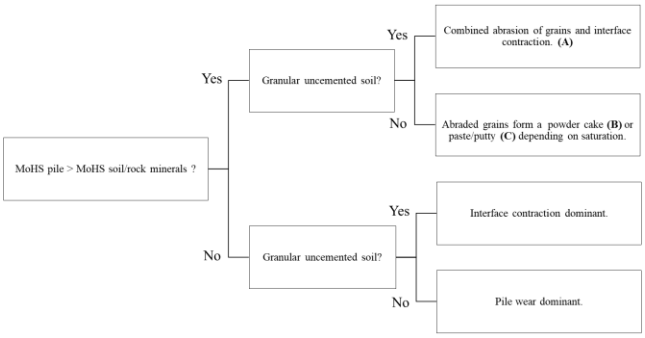

Fig.1. Schematic overview of processes and wear mechanisms at the pile-soil interface. This paper provides theory behind mechanisms A, B and C.

3 A GENERAL MODEL FOR WEAR AND FRICTION AT THE PILE-SOIL INTERFACE

3.1 Wear at the soil-pile interface

The theory developed in this paper holds for the cases where the pile material hardness is larger than the rock or soil mineral hardness. Basically, all sliding wear processes follow the Archard wear equation (Archard, 1953):

$$V = k \cdot F_n \cdot s \tag{1}$$

Eq.1 describes the fundamental relation between the worn volume V in m^3, which is proportional to the sliding distance s in m and the normal load between the two sliding surfaces F_n in N. They are related via the specific wear rate k in m^3/Nm of the material that is subject to wear (the softer material).

Since abrasive wear is directly proportional to the relative displacement of two materials, there is only an indirect relation with piling rate: the larger the rate, the larger the relative displacement per unit of time. The determining factor however is the relative displacement, which means that the theory developed in this paper is universally applicable to any pile driving technique.

The specific wear rate k is independent of the stress state of the material, it is an engineering property which can be determined with well-controlled laboratory experiments. Eq.1 provides a general physical model for wear (both applicable to adhesive wear as in clay and abrasive wear as in rock). The model parameters could be determined for any pile material in relation to any rock or soil sample under laboratory conditions, very similar to the CNS tests (Poricini. 2003; Doughty et al., 2018; Chan et al. 2019). In this paper we focus on the non-cohesive soils and rock.

We consider a soil or rock body being penetrated by a pile down to $z = z_{end}$ m, Fig.2. The pile penetrates with an average penetration velocity of u m/s. The total displacement s experienced by a soil layer at horizon $0 < z < z_{end}$ m after t s of driving is then given by:

$$s(z,t) = 0 \qquad 0 \le t < \frac{z}{u} \tag{2}$$

$$s(z,t) = u \cdot t - z \qquad \frac{z}{u} \le t \le \frac{z_{end}}{u}$$

The normal force at the interface follows from the effective radial stress:

$$F_n(z) = \sigma_r'(z) \cdot \pi \cdot D \cdot dz \tag{3}$$

With σ_r' the effective radial stress as function of z, D the pile diameter and dz the depth increment in the soil body along which the normal force is determined.

The abraded volume of material of a soil layer with thickness dz at horizon z during penetration follows from Eqs.1-3:

$$V(z,t) = \sigma_r'(z) \cdot \pi \cdot D \cdot k(z) \cdot s(z,t) \cdot dz \tag{4}$$

V is the volume of material that is abraded from the virgin soil/rock due to the sliding of the pile, not to be confused with the volume displaced by the pile itself. Note that in Eq.4 the radial stress and specific wear rate k will vary along the coordinate z due to the presence (potentially) of different soil layers with different properties.

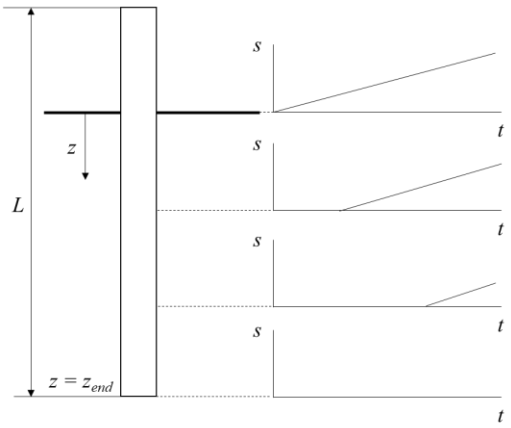

Fig.2. Coordinate system of a pile penetrating the soil with (in this example) a constant penetration speed u. $z = 0$ is ground level, positive downward. The total pile displacement s experienced at a certain horizon z is given by Eq.2.

The abraded material will fill the gap between the pile and soil body and due to the high stresses, debris will be grinded to very small sizes. This can lead to local densification and in the presence of sufficient water, a paste-like material will form. When assuming all

material remains at the pile-soil interface, the layer thickness h of the worn material can be estimated as $h \approx V/(\pi \cdot D \cdot dz)$. The permeability of the paste or abraded rock will be very small or even negligible, and the soil/rock deformation at the interface can be considered an undrained process.

The interface layer thickness h will not grow infinitely and after a certain displacement s, a critical layer thickness h_{crit} is reached, after which further growth is assumed to stop. As working hypothesis, a relation between the effective radial stress and the development of the interface layer is introduced, which holds for dry and saturated conditions. We propose an inversely proportional relationship between σ_r' and h until the critical layer thickness is reached. For dry conditions, the specific wear rate remains constant as a material property and the radial stress is assumed to reduce as a result of the interface layer being denser than the original soil/rock matrix (for relatively porous rock only), according to:

$$\sigma_r'(z,h) = \sigma'_{r,0}(z) \cdot (1 - h(z)/h_{crit}) \quad (5)$$

With $\sigma'_{r,0}$ the initial radial effective stress at the onset of the abrasive wear process.

For saturated conditions, the stress state will change initially, but the paste layer will also act as a lubricant and actually reduce the wear potential of the pile. The latter effect is assumed to be dominant, and it is included by reducing the specific wear rate in a similar fashion as was done for the radial stress:

$$k(z) = k_0(z) \cdot (1 - h(z)/h_{crit}) \quad (6)$$

Substitution of Eq.5 or Eq.6 in Eq.4 and dividing by $(\pi \cdot D \cdot dz)$ gives the expression for the development of the interface layer thickness at horizon z as a function of time t for all soil horizons $0 < z \leq z_{end}$, which is valid for both dry and saturated conditions:

$$h(z,t) = \sigma'_{r,0}(z) \cdot k_0(z) \cdot s(z,t) \cdot \left(1 + \frac{\sigma'_{r,0} \cdot k_0(z) \cdot s(z,t)}{h_{crit}}\right)^{-1} \quad (7)$$

The critical layer thickness is a theoretical concept but experimental data exists for development of abraded interface layers for different types of sand (Ho et al., 2011) and chalk (Buckley, 2018; Muir Wood et al., 2015). For sand (quartz)–steel interfaces we have comparable hardness with two-body wear, while in chalk-steel interfaces the steel pile roughness is dominant. The dominant length scale for pure abrasion (infinite surfaces, no boundary effects) is the pile material roughness R_a in m, and for pile driving with open ended piles, the dominant length scale of the cracks and debris at the pile tip will be in the order of the pile wall thickness and this determines the extent of chalk remoulding. Two length scales play a role in pile driving in weak rocks: the actual abrasion and development of an interface layer (R_a dominated) and secondary remoulding (pile wall thickness). Abrasion will result in the development of the interface and we therefore define the critical layer thickness relative to the surface roughness of the pile:

$$h_{crit} = N \cdot R_a \quad (8)$$

With $N \approx 10$ as a first estimate.

We will explore the case of a saturated interface layer further in the next section.

3.2 Shear stresses and friction at the pile soil interface under saturated conditions

Under perfectly dry conditions, the shear stresses between the pile wall and the soil body are described by Coulomb friction $\tau = \sigma_r' \cdot \tan\delta$, with τ the shear stress in Pa en δ the friction angle between the steel and the soil body in degrees. The paste interface layer developing under saturated conditions will most probably show non-Newtonian behavior, and depending on the actual mineral composition of the rock or soil formation of interest, different rheology can be expected from case to case. For chalk, strain hardening (Doughty et al., 2018) and thixotropy (negligible during pile driving) are known to play a role in the increase in post-installation axial capacity (Chan et al., 2019). The effect of ambient pressure on rheology of water and pastes is only small (Först et al. 2000; Kim et al. 2017), and can be neglected. Here we assume Bingham rheology, characterized by a yield stress and Newtonian behavior once the yield stress is exceeded, i.e. no strain hardening:

$$\tau = \tau_y + \mu \cdot \dot{\gamma} \quad (9)$$

With τ_y the paste yield stress in Pa, μ the paste viscosity in Pas and $\dot{\gamma} \approx u/h_{crit}$ the shear rate. During the initial stage of pure abrasion with $h_{crit} \approx 10 \cdot R_a$, the shear rate will be much larger than for the fully remoulded zone (with h_{crit} in the order of the pile wall thickness). The viscous contribution to the friction between the pile and the soil thus decreases, and the actual friction decreases as the interface layer grows beyond the critical layer thickness due to secondary effects described in Section 3.1.

The friction angle is defined as $\tan\delta = \tau/\sigma_r'$. The friction angle δ_p in the case of a paste layer could be understood as a Coulomb-equivalent:

$$\tan\delta_p = \frac{\tau}{\sigma_r'} = \frac{\tau_y + \mu\cdot\dot{\gamma}}{\sigma_r'} \quad (10)$$

The gradual transition from Coulomb friction to rheology dominated shaft friction can be described by relating the interface friction angle δ to the development of the layer thickness h (Eq.7), see Fig. 3. At zero layer-thickness it holds $\tan\delta\,(h=0) = \tan\delta_0$, with δ_0 being the friction angle between the virgin soil or rock and the pile without any intermediate layer. When the layer is fully developed to h=h_{crit}, we get $\delta(h = h_{crit}) = \delta_p$ with δ_p the friction angle of the paste defined by Eq.10. With h a function of z and t, $\tan\delta(z,t)$ then can be written as:

$$\tan\delta\,(z,t) = \tan\delta_0 \cdot \left(1 - \frac{h(z,t)}{h_{crit}}\right) + \tan\delta_p \cdot \frac{h(z,t)}{h_{crit}} \quad (11)$$

Or alternatively when substituting Eqs.7 and 8:

$$\frac{\tan\delta(z,t)}{\tan\delta_0} = \frac{\sigma_r'\cdot k_0}{\frac{10\cdot R_a}{s(z,t)} + \sigma_r'\cdot k_0} \cdot \left(\tan\delta_p - 1\right) \quad (12)$$

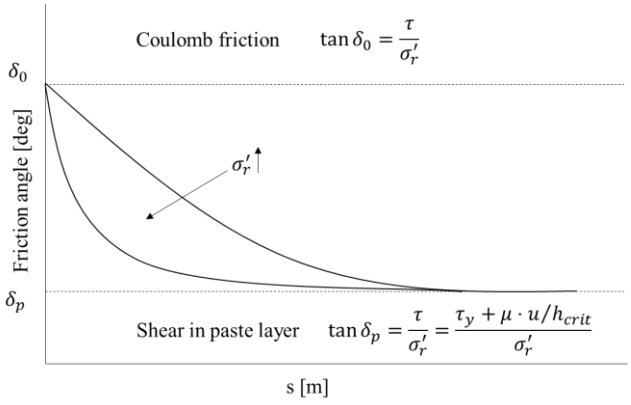

Fig.3. Coulomb friction and its rheology-equivalent used to describe the transition towards paste layer dominated friction at the pile-soil interface. Larger radial stresses at the pile indicate quicker development towards a paste layer.

4 VALIDATION WITH EXPERIMENTAL DATA

Eq. 12 is validated with three case studies from literature comprising steel-calcareous sands interface testing (Tabucanon, 1997), steel-chalk interface testing (Ziogos et al., 2016) and pile driving in saturated calcareous sands (Denes, 2016).

4.1 Steel-calcareous sands interface tests (dry)

Tabucanon (1997) reports on dry shear tests (cyclic and monotonic) on silica sand and calcareous sands. Grain effects dominated the results of cyclic loading with small displacement for both sands. However, CNS (~227 kPa/mm) ring shear tests (monotonic shearing over 3 m) showed appr. constant stresses in the order of 50-150 kPa for silica sands, while for the calc. sands both normal and shear stress reduced towards almost zero. This was ascribed to continued compression under loading and the crushing of the particles, a dry abrasive wear process.

We used R_a = 10 µm, δ_0 = 33°, δ_p = 2.9°, 0 < s ≤ 3.2 m, σ_r' = 236 kPa, k_0 = 0.15 10^{-8} m^3/Nm (low wear scenario) and k_0 = 0.50 10^{-8} m^3/Nm (high wear scenario) to study Eqs. 5, 7 and 11, see Figs 4 and 5. The specific wear rate should be seen in conjunction with the surface roughness of the steel samples, since they both determine the worn volume. The model captures the stress development well.

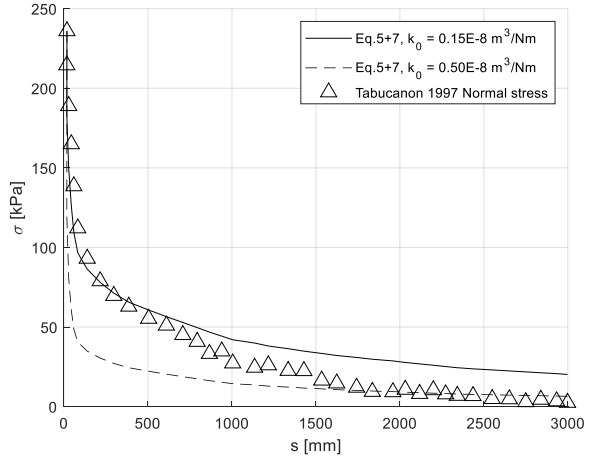

Fig.4. Reduction of the normal stress in Tabucanon's ring shear tests (CNS) of calcareous sands as a result of the development of a powder cake at the interface.

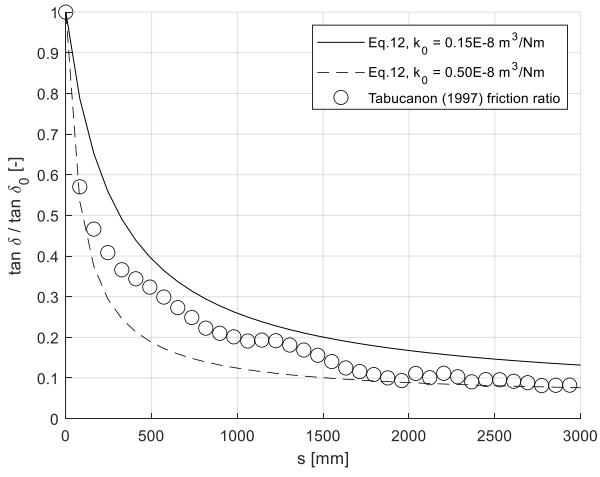

Fig.5. Reduction of the interface friction angle ratio in Tabucanon's ring shear tests (CNS) of calcareous sands as a result of the development of a powder cake at the interface.

4.2 Saturated chalk-steel interface shear test

Ziogos et al. (2016) studied interface friction between rock and steel samples under constant normal

loading (at different magnitudes) for sliding distances up to 7 m. For chalk it was observed that at the onset of significant surface wear the interface friction coefficients went down to almost half the chalk-chalk friction coefficient. They found a powdered interface layer for dry samples and a paste film on the interface for saturated chalk samples.

The saturated chalk data is plotted in Fig.6 together with Eq.12 using the input parameters R_a = 7.2 µm, δ_0 = 30.5º, δ_p = 10º, $0 < s \leq 7$ m, $\sigma_{r,0}'$ = 700 kPa, k_0 = 0.4 10^{-10} m^3/Nm (estimated to fit the data). Eq.12 proved to be very sensitive to k_0 and δ_p. In the absence of specific wear rates and rheological data, both parameters were estimated to provide a good fit. The value of δ_p was checked with the associated shear stress that would be obtained from Eq.10 ($\tau \approx 120$ kPa which seems reasonable).

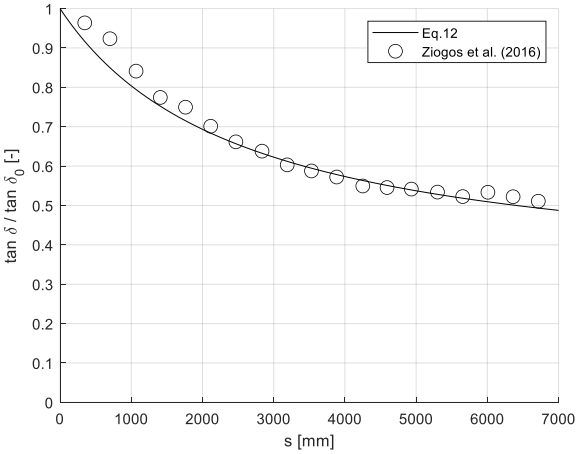

Fig.6. Eq.12 plotted with the data of Ziogos et al. (2016) for abrasive wear of saturated chalk at 700 kPa normal pressure.

4.3 Pile driving in saturated calcareous sand

Denes (2016) has analyzed a D = 0.508 m pile driven in calcareous sand, consisting of both cemented and uncemented layers, with penetration to a depth of 39 m.

Calcareous sands are sensitive to abrasion and pile driving took place in saturated conditions so a combination of mechanisms A and C is expected (see Fig. 1). It is unknown whether a paste layer formed.

In Fig. 7 the percentage of shaft friction loss as reported in Denes (2016) is converted to the ratio of friction coefficients (1 for 0% loss 0 for 100% loss). The relative displacement is converted to the actual displacement at the respective soil horizons. With homogeneous rock properties one would expect the data of the three horizons to fall onto the same line in Fig.7. This seems to be the case for the 5 m horizon (up to a displacement of 12 m) and the 15 m horizon data, and for the 5 m horizon data (from 12 m displacement onward) and the 25 m horizon data.

It can be seen in Fig.7 that Eq. 12 follows the trends in the data well for R_a = 3.5 µm, δ_0 = 30º, $\tan\delta_p/\tan\delta_0 = 0$, $0 < s \leq 35$ m, σ_r' = 48 kPa, k_0 = 0.7 10^{-10} m^3/Nm (low wear scenario) and k_0 = 2.50 10^{-10} m^3/Nm (high wear scenario). It should be noted that the results are very sensitive to the input data, emphasizing the need for laboratory testing in conjunction with use of the model.

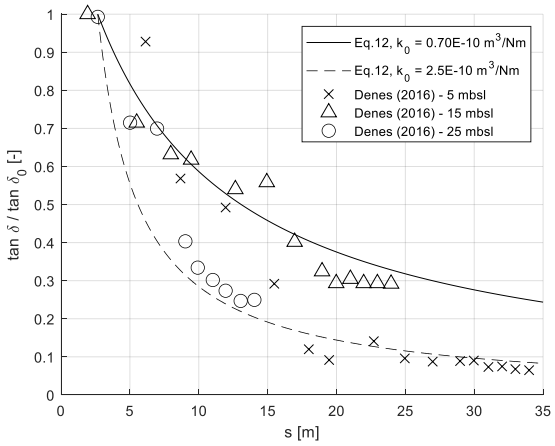

Fig.7. Eq.12 plotted with the data of Denes (2016) for pile driving in calcareous sands for two different specific wear rate scenarios.

5 CONCLUSIONS AND RECOMMENDATIONS

Based on wear theory, the relative hardness of pile and rock/soil is expected to play an important role in the physics governing friction fatigue of weak rock and soft (cemented) non -cohesive soils (‘weak rock’). Abrasion in these cases is expected to be dominant over grain contraction at the pile-soil interface. Depending on the degree of saturation of the rock/soil, a powder cake or paste layer will form, which shows a direct relation between layer thickness growth and sliding distance.

Under assumption of an inversely proportional relation between the wear rate and the interface layer thickness, a model is presented for the transition from virgin rock-steel interface dominated friction to a friction situation dominated by the interface layer properties. In case of a paste interface, the rheology of the paste is governing. For known rheology an accurate description of shear stress as function of penetration speed can be given. The model parameters are all physical parameters that can be determined in a laboratory with standard geotechnical testing methods or rheometry.

The model is validated with three datasets from literature comprising calcareous sand-steel ring shear

tests, chalk-steel interface friction tests and friction fatigue as determined in pile driving in calcareous sands. The model correctly describes the trends of friction reduction in all cases. In absence of data on the specific wear rates of the different types of soil and rock, the specific wear rates in these cases were chosen to give a good quantitative fit to the measurement data.

In future work it is planned to validate the model with a well-documented pile driving case, preferably in chalk, of which also the interface paste-material properties are known.

ACKNOWLEDGEMENTS

The work presented in this paper is sponsored by IQIP, The Netherlands.

REFERENCES

1) Alm, T. and Hamre, L. (2001). Soil model for pile driveability predictions based on CPT interpretations. P.1297-1302.

2) Archard, J.F. (1953). Contact and rubbing of flat surfaces. Journal of applied Physics 24, 981.

3) Barrett, J.W. and Prendergast, L.J. (2020). Empirical shaft resistance of driven piles penetrating weak rock. Rock Mechanics and Rock Engineering 53, p.5531-5543.

4) Beijer-Lundberg, A. (2009). Displacement pile installation effects in sand – an experimental study. PhD thesis, Delft University of Technology.

5) Buckley, R.M. (2018). The axial behavior of displacement piles in chalk. PhD thesis, Imperial College London, UK.

6) Chan, L.D.; Buckley, R.M., Liu, T. and Jardine, R.J. (2019). Laboratory investigation of interface shearing in chalk. Proceedings of the 7th international symposium on deformation characteristics of geomaterials. Glasgow UK.

7) Gavin, K.G. and O'Kelly, B.C. (2007). Effect of friction fatigue on pile capacity in dense sand. Journal of Geotechnical and Geoenvironmental Engineering, p.63-71.

8) Denes, D. (2016). Observing friction fatigue on calcareous material. Geotechnical and Geophysical Site characterization. Eds. Lehane, Acosta-Martinez and Kelly. p.1199-1204.

9) Doughty, L.; Buckley, R.M. and Jardine, R.J. (2018). Laboratory testing of chalk. Engineering in chalk: proceedings of the chalk 2018 conference. ICE, London.

10) Dührkop, J.; Maretzki, S. and Rieser, J. (2017). Re-evaluation of pile driveability in chalk. Proceedings of the 8th international Conference on Offshore Site Investigation and Geotechnics, 12-14 September 2017, London.

11) Först, P., Werner, F. and Delgado, A. (2000). The viscosity of water at high pressures – especially at subzero degrees centrigrade. Rheol. Acta 39, 566-573.

12) Hancock, B.C. (2018). The wall friction properties of pharmaceutical powders, blends, and granulations. Journal of Pharmaceutical Sciences 8:1.

13) Heerema, E.P. (1980). Predicting pile driveability: Heather as an illustration of the "friction fatigue" theory. Ground Engineering April 1980, p.15-20.

14) Hobbs, N.B. and Atkinson, M.S. (1993). Compression and tension tests on open-ended tube pile in chalk. Ground Engineering 26, no. 3, p.31-34.

17) Kim, J.H., Kwon, S.H., Kawashima, S. and Yim, H.J. (2017). Rheology of cement paste under high pressure. Cement and concrete composites 77, 60-67.

18) Maynard, A.W.; Hamre, L.; Butterworth, D. and Davison, F. (2019). Improved pile installation predictions for monopiles. 10th international conference on stress wave theory and testing methods for deep foundations. San Diego, USA.

19) Muir Wood, A.; Mackenzie, B.; Burbury, D.; Rattley, M.; Clayton, C. R. I.; Mygind, M.; Wessel Andersen, K.; Le Blanc Thilsted, C. and Albjerg Liingaard, M. (2015). Design of large diameter monopiles in chalk at Westermost Rough offshore wind farm. Proc. 3rd Conf. Frontiers in Offshore Geotechnics, Oslo, Norway: 723-728.

15) Hutchings, I. and Shipway, P. (2017). Tribology – friction and wear of engineering materials, second edtion. Butterworth-Heinemann.

16) Jardine, R.J.; Buckly, R.M.; Kontoe,S.; Barbosa, P. and Schroeder, F.C. (2018). Keynote lecture: behavior of piles driven in chalk. International conference on Engineering in Chalk 2018, British Geotechnical Association.

20) Poricin, D.; Fioravante, V.; Nicola Ghionna, V. and Pedroni, S. (2003). Interface behavior of sands from constant normal stiffness direct shear tests. Geotechnical Testing Journal 26, no.3, p.1-13.

21) Poulos, H.G. (2000). Some aspects of pile skin friction in calcareous sediments. Engineering for calcareous sediments. Al-Shafei (ed). Balkema, Rotterdam.

22) Tabucanon, J.T. (1997). Shaft reduction of piles in sand. PhD thesis, The University of Sydney.

23) Terente, V.; Irvine, J.; Comrie, R. and Crowley, J. (2015). Pile driving and pile installation in weak rock. European Conference on Soil Mechanics & Geotechnical Engineering XVI.

24) Terente, V.; Torres, I.; Irvine, J. and Jaeck, C. (2017). Driven pile design method for weak rock. Design of Piles in Weak Rock - follow up paper - SUT conference, London.

25) White, D.J. and Lehane, B.M. (2004). Friction fatigue on displacement piles in sand. Géotechnique 54, no. 10, 645-658.

26) Ziogos, A.; Brown, M.; Ivanovic, A.; and Morgan, N. (2016). Chalk-steel interface testing for marine energy foundations. Geotechnical Engineering.